Nuclear Instruments and Methods in Physics Research B37/38 (1989) 923–929
North-Holland, Amsterdam

IMPLANTATION, DAMAGE, AND REGROWTH OF HIGH T_c SUPERCONDUCTORS

Alice E. WHITE, K.T. SHORT, J.P. GARNO, J.M. VALLES, R.C. DYNES, L.F. SCHNEEMEYER, J. WASZCZAK, A.F.J. LEVI, M. ANZLOWAR and K.W. BALDWIN

AT&T Bell Laboratories, Room 1E-433, 600 Mountain Ave., Murray Hill, NJ 07974, USA

We have observed superconductivity in thin films of $(La_{1-x}Sr_x)_2CuO_y$ which are fabricated by implanting evaporated La/Cu multilayer films with Sr and annealing in oxygen. The films are insulating and partially transparent as-implanted, but they darken and become conducting at annealing temperatures as low as 500 °C. The resistive behavior is very sensitive to the annealing conditions and the superconducting layer appears to be buried beneath the surface. Similarly, implantation of F, O, and Ne into single crystals and high quality ($\chi_{min} < 30\%$) thin films of $YBa_2Cu_3O_{7-\delta}$ creates a buried damage layer and renders the films insulating. From Rutherford backscattering and channeling analysis, we find that some regrowth of the damaged layer does occur on subsequent annealing. Studies of the transport properties of these films as a function of MeV-ion-beam-induced damage show that the critical current can be controllably reduced at low fluences. The metal-to-insulator transition, which occurs at higher fluences, seems to result from a reduction in carrier mobility rather than carrier freeze-out.

1. Introduction

As thin films and single crystals of the new high T_c oxide superconductors become available, ion beams are playing a significant role in materials modification and analysis. We have used implantation of keV ions to fabricate thin films of these superconductors and irradiation with both keV and MeV ions to controllably introduce defects into epitaxial thin films as well as single crystals. The first section of this paper will concentrate on the fabrication: in addition to demonstrating the feasibility of using implantation of keV ions into evaporated multilayer films to make these superconductors, we experimented with tuning the stoichiometry of a superconducting film by implantation. This proved more difficult than expected in films of $YBa_2Cu_3O_{7-\delta}$ due to preferential sputtering of Ba. The films were extremely sensitive to implantation damage as well as annealing conditions, so we also performed some experiments designed to explore the regrowth of the damage with annealing. The regrowth studies are described in the second section. As well as causing structural changes, the ion damage also has a profound effect on the transport properties of these films. Low ion fluences can be used to controllably reduce critical currents and higher ion fluences cause a metal-to-insulator transition which can be probed with temperature-dependent resistivity and Hall effect measurements. These results are presented in the last section.

2. Synthesis of $(La_{1-x}Sr_x)_2CuO_y$ films with ion implantation

Although bulk polycrystalline ceramic pellets of the high T_c oxide superconductors are relatively straightforward to make [1], the fabrication of thin films has been troublesome [2]. The problems stem mainly from the chemical reactivity of the various constituents which means that they are hard to deposit. Furthermore, they react with most common substrate materials (especially silicon and sapphire) and they are prone to phase segregation and selective oxidation. Drawing on our experience with ion beam synthesis, in which we implant stoichiometric concentrations of one constituent into a substrate of the other constituent and anneal to form a compound [3], we started with an evaporated multilayer film of La and Cu, implanted Sr, and annealed to form what turned out to be a buried layer of superconducting $(La_{1-x}Sr_x)_2CuO_y$.

Alternating layers of La and Cu, each approximately 100–200 Å thick, were evaporated thermally onto a (100)-oriented sapphire substrate at 10^{-7} Torr without breaking the vacuum. The individual layer thicknesses were chosen so that the La and Cu would be present in the proper atomic ratios and the final film thicknesses were ~ 2000 Å. A Rutherford backscattering (RBS) spectrum (fig. 1a) of the as-deposited film confirmed the atomic ratios and showed the presence of a surface oxide. The energy (150 keV) and fluence (1.5×10^{16} Sr^+/cm^2) of the Sr implantation were chosen so the peak of the implant profile would fall roughly in the center of the film and the total concentration, integrated over the entire film, would give the correct stoichiometry. Following implantation, the films were insulating, but, after an anneal at > 500 °C in flowing dry O_2, they showed evidence of superconductivity. The Sr shows up clearly in the RBS spectrum of the annealed film (fig. 1b), and, although the Sr does not redistribute much during the anneal, the final concentrations of each constituent are

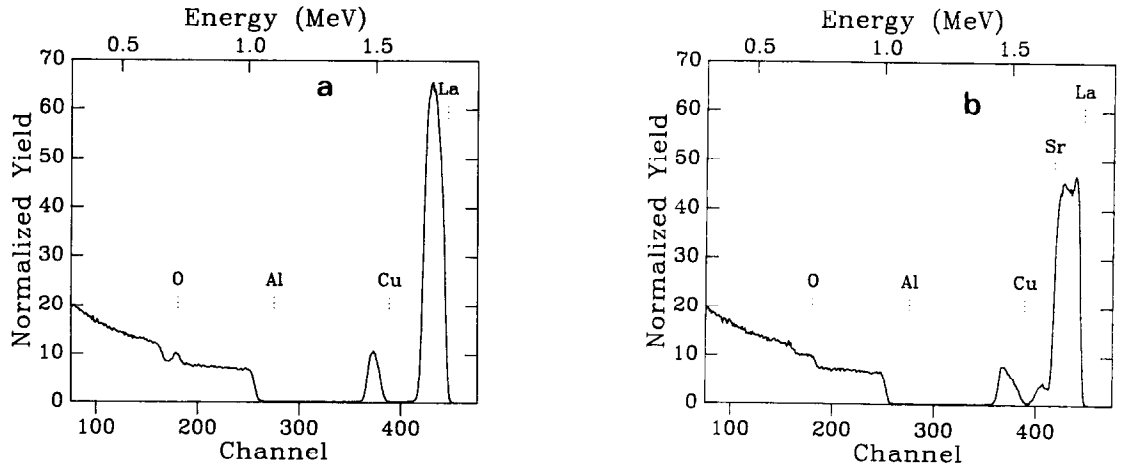

Fig. 1. (a) RBS spectrum (2 MeV He^+, 170°) of an as-deposited La/Cu multilayer film with a thin surface oxide on (100) sapphire. The atomic concentrations are ~ 50 at.% La and ~ 20 at.% Cu. (b) RBS spectrum of the film from (a) after implantation of 1.5×10^{16} Sr^+/cm^2 at 150 keV and annealing at 500°C in flowing O_2 for 2 h. The film is now fully oxygenated and the atomic concentrations are 26 at.% La, 2 at.% Sr, 14 at.% Cu, and 57 at.% O.

close to the desired stoichiometry.

The resistance characteristics of the films were measured by attaching gold leads in a four terminal configuration to the film surface with silver paint. These could be easily removed with acetone for subsequent anneals. The superconducting transitions observed illustrate the possibilities of this technique, although the resistance does not drop completely to zero. We believe this is because the superconducting layer is actually buried beneath the surface of the film and so there is always a nonzero resistance in series. The $(La_{1-x}Sr_x)_2CuO_y$ films made by sputtering or evaporation were found to degrade readily on exposure to air [2], but the films described here are fairly robust, perhaps because they have a natural capping layer.

Resistive transitions for a sequence of anneals on a representative film are shown in fig. 2. After implantation, the samples were inserted into a hot tube furnace with flowing O_2 for a set time and quenched to room temperature. Since the contact geometry changed between measurements, the relative resistances are not directly comparable; however, the resistance ratio, defined as $R(300\ K)/R(100\ K)$, is geometry independent. A 1 h anneal at 500°C transforms the film from insulating to superconducting, with a metallic-like R vs T curve that shows a superconducting onset at ~ 40 K and a broad resistive transition. Annealing at 580°C for an additional hour does not affect the resistance ratio, but raises the superconducting onset temperature slightly and sharpens the transition. The film starts degrading with higher temperature anneals (and rapid cooldowns), presumably due to loss of oxygen [4]. After an additional hour at 720°C, the resistance ratio of the film is nearly 1, and after another hour at 900°C, the film is insulating at room temperature. This film was subsequently rejuvenated by performing a lower temperature anneal (440°C) to increase the oxygen content. The resistive curve of the film after this anneal hinted of semiconducting behavior, but had a definitive superconducting transition with an onset at ~ 30 K.

Although the conditions have not been optimized, these experiments have demonstrated that implantation is a feasible technique for synthesizing superconducting films. Similar results have recently been reported for the Y implantation into Ba/Cu multilayers by Nastasi et al.

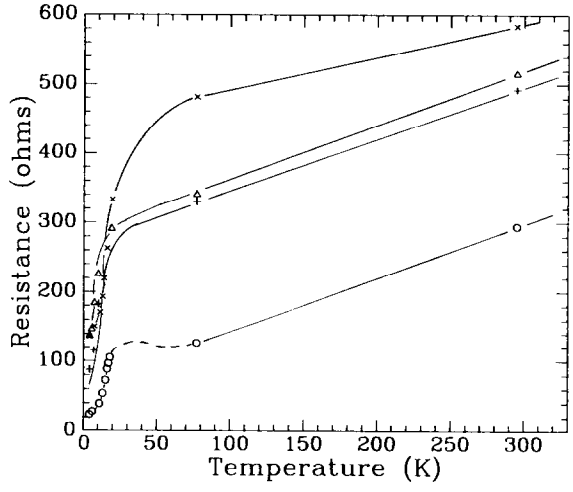

Fig. 2. R vs T plots for a $(La_{1-x}Sr_x)_2CuO_y$ film fabricated by implantation into an evaporated La/Cu multilayer sandwich. The anneal sequence was: 500°C for 1 h (open triangles), 580°C for 1 h (crosses), 720°C for 1 h (×'s), 900°C for 1 h (insulating), and 440°C for 1 h (circles).

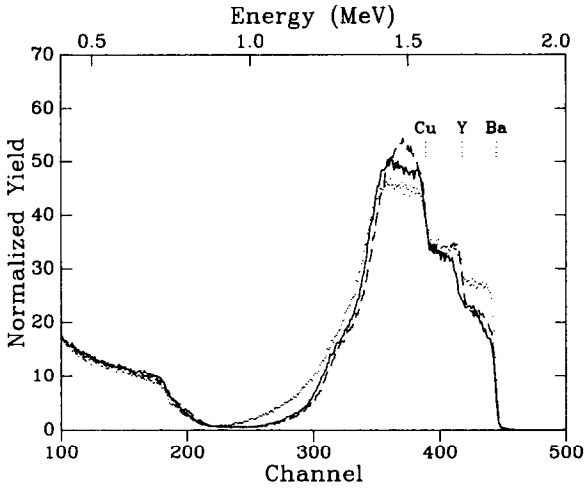

Fig. 3. Random RBS spectra for a Cu-poor film on sapphire after annealing (dotted line), after implantation with 1×10^{17} /cm^2 180 keV Cu^+ (dashed line), and after a second annealing (solid line). Although the Cu concentration is increased by implantation, Ba is sputtered preferentially.

[5]. Since the Sr shows limited redistribution, we obtain a naturally capped film. Thickness of the initial multilayer film was limited to ~ 2000 Å by the energy (and therefore the depth) of the implant – we expect that MeV beams will provide much more versatility. These experiments also illustrated the sensitivity of the electrical properties of the films to ion damage; they become insulating at relatively low ion fluences. Moreover, we found that the oxygen content of these films could be altered (changing them from superconducting to insulating) by varying the annealing conditions.

An attempt to modify the stoichiometry of a Cu-poor film by implantation of Cu was less successful as illustrated in fig. 3. The starting film was deposited on sapphire by simultaneously evaporating BaF_2, Y, and Cu from three sources in 10^{-5} Torr O_2 to a thickness of ~ 5000 Å [6]. After the standard annealing cycle, the stoichiometry as determined by RBS was $Y_{1.0}Ba_{2.0}Cu_{2.6}O_x$. Again, the implant fluence (1×10^{17} Cu^+/cm^2) was chosen to give the correct concentration when integrated over the film. In fig. 3, the increase in the Cu concentration from the implantation is clearly visible; however, the Ba has been preferentially sputtered giving a stoichiometry of $Y_{1.0}Ba_{0.8}Cu_{3.0}O_x$. After annealing at 750 °C and then at 440 °C each for 1 h, the Cu is uniformly distributed throughout the film, but the loss of Ba means that the film is not superconducting.

3. Damage recovery of single crystals and thin films

One of the reasons that implantation is so useful for doping semiconductors is that the damaged region can be recrystallized with a low temperature anneal (500 °C), using the substrate as a seed. If implantation is to be used to tailor the electrical properties of these superconductors, we need to explore the damage recovery. For example, do they regrow epitaxially, layer by layer, as do the semiconductors? Stoffel et al. [7] recently reported results on amorphization and thermal annealing of $YBa_2Cu_3O_{7-\delta}$ single crystals. The amorphization was accomplished with implantation of 30 keV O^+ to a fluence of 1×10^{15} /cm^2. Channeling on the implanted crystals showed that the disordered layer extended to a depth of 700 Å. However, upon annealing, loss of Ba was observed, presumably through surface segregation and sublimation. Since our experience with annealing of surface and buried damaged layers indicated that the presence of an amorphous surface layer most likely accelerated the loss of Ba, we repeated the experiment on both single crystals and oriented thin films of $YBa_2Cu_3O_{7-\delta}$ using implantation conditions designed to bury the damage. In this way, we were able to observe re-ordering of the superconductor, although evidence suggests that the re-ordering arises from grain growth rather than solid phase epitaxy.

The single crystals, which form with a layered structure (perpendicular to the c-axis), were prepared from yttrium oxide–barium oxide–copper oxide melts [8]. They were then mechanically separated from the flux. Crystals averaging 2–4 mm^2 were chosen for this study. Channeling measurements of these crystals showed χ_{min}'s of 3–5%, similar to the previously reported χ_{min}'s [7]. Implantation energies for F^+, O^+, and Ne^+ were chosen so that the projected range and straggle would place the damage below the surface. Although we cannot be absolutely certain that the damaged region was amorphous, comparison of channeled and random RBS yields after the implantation showed a subsurface region of complete disorder and a surface χ_{min} of ~ 90%.

Furnace anneals were performed in flowing oxygen, again with a quench to room temperature. Fig. 4 shows a sequence of channeling spectra from a 200 keV, 6×10^{14} /cm^2 F^+ implant, illustrating the gradual recovery of the crystallinity in the damaged region. Longer anneals at low temperatures did not result in significantly lower χ_{min}'s, and it was necessary to go to high temperatures (800 °C) to get ~ 50% recovery. From this, we conclude that most of the recovery of crystallinity does not occur by monolayer by monolayer growth (solid phase epitaxy); rather, the order is probably restored by annealing of defects and preferential growth of oriented grains. It is difficult to judge the relative recovery of the Y, Ba, and Cu sublattices because of the overlap of the respective regions of the spectrum, but it does appear that the Ba and Cu sublattices show better recovery than the Y sublattice.

By performing similar studies in oriented thin films of $YBa_2Cu_3O_{7-\delta}$ on (100) $SrTiO_3$ substrates [6], we

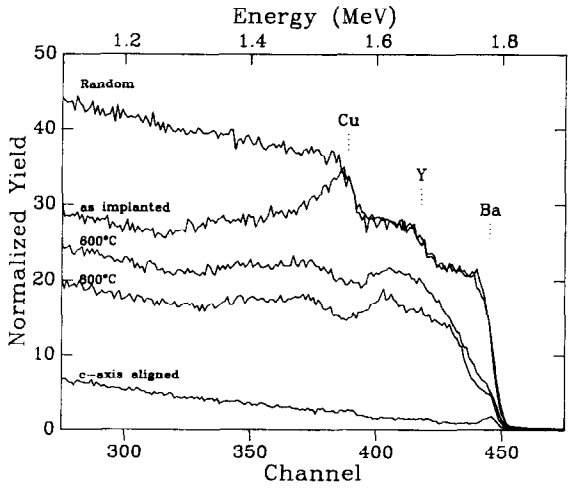

Fig. 4. Random and channeled RBS spectra illustrating the recovery of a single crystal of $YBa_2Cu_3O_x$ after implantation of 6×10^{14}/cm^2 200 keV F^+ (to create a subsurface damaged layer) and annealing at 600 °C and 800 °C each for 1 h. Before implantation, the channeled spectrum shows $\chi_{min} = 3\%$.

were able to monitor the changes in the electrical properties of the films through the damage and recovery process as well. For the implantations, we again chose a 200 keV F^+ beam to maintain the surface crystallinity. As seen in fig. 5, the recovery with annealing proceeded much the same way as in the single crystals, although the spectra are more difficult to interpret because of the overlap of the Cu and Sr regions. There is a hint that

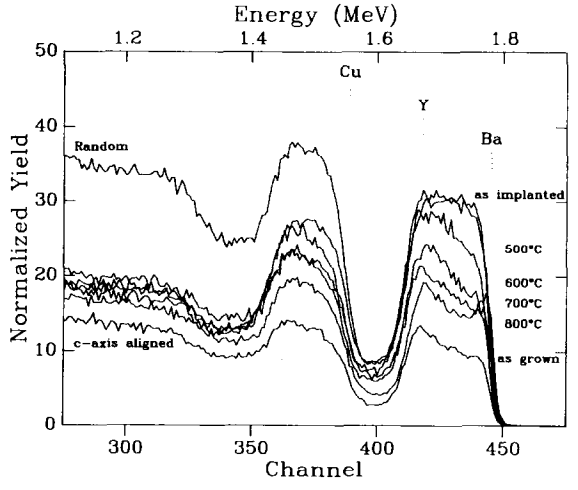

Fig. 5. Random and channeled RBS spectra for an oriented thin film of $YBa_2Cu_3O_x$ on $SrTiO_3$ after implantation with 4×10^{14} /cm^2 200 keV F^+ and an annealing sequence of 500 °C, 600 °C, 700 °C, and 800 °C each for an hour. Before implantation the film has $\chi_{min} = 32\%$, after implantation it is almost completely disordered except for the surface, and after the anneals the χ_{min} has recovered to 50%.

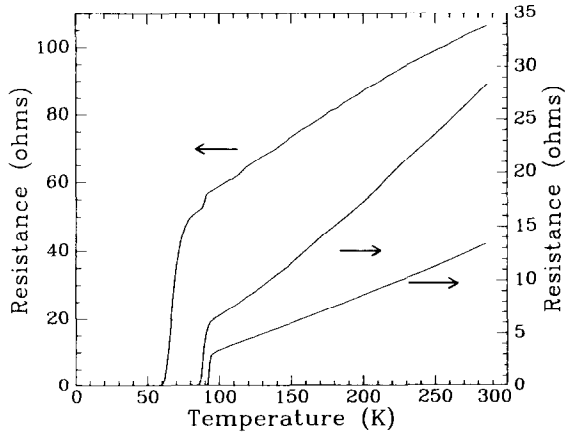

Fig. 6. R vs T plots for the sample in fig. 5. The lowest curve was measured on a piece of the film before implantation and annealing; the middle curve was measured on the half of the film that was not implanted, but received the annealing sequence; and the upper curve was measured on the region of the film that was implanted (insulating) and annealed. Since the contact geometries differed in the three measurements, the resistances cannot be compared.

the regrowth starts at the surface, which is much less heavily damaged than the film/substrate interface. Regardless, even the undamaged film shows more dechanneling at the back interface than at the surface.

Fig. 6 shows the results of the electrical measurements for the sample in fig. 5. The lower curve was taken before the implantation and shows a fairly linear normal state $R(T)$ dependence and $T(R = 0)$ at 92 K. After implantation, the implanted region of the film has a distinctly greenish hue and is insulating at room temperature. Dramatic recovery of the superconductivity occurs on annealing as seen in the upper R vs T characteristic in fig. 6. The resistances of the films are not comparable because of differences in the measuring geometries, but $T(R = 0)$ has risen to 56 K and the resistance ratio is greater than 1. The hump in the resistive transition has been previously observed in films that have been irradiated with MeV ions [10] and can be interpreted as evidence for the presence of another superconducting phase. For comparison, a region on the film which was not implanted but received the same annealing sequence was also measured (middle curve). This region showed a pronounced positive curvature in the R vs T characteristic and a slightly degraded $T(R = 0)$ of 86 K, both suggestive of the recently identified Cu-rich phase, $Y_2Ba_4Cu_8O_{20-\delta}$ [6,9].

4. Ion-beam-induced changes in transport properties

Although the physical mechanisms for superconductivity in the new high T_c oxide superconductors are not

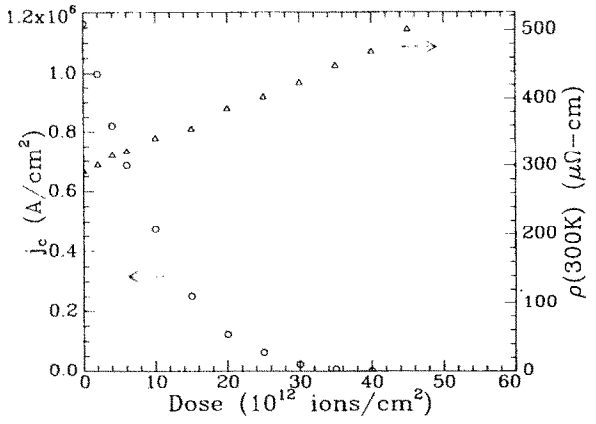

Fig. 7. Change in J_c and $\rho(300\ \mathrm{K})$ of an oriented thin film of $YBa_2Cu_3O_x$ due to ion irradiation with low fluences of 1 MeV Ne^+. At 4.0×10^{13} ions/cm^2, J_c has dropped three orders of magnitude.

yet understood, many of the important practical properties, such as the critical current density, J_c, depend on the extrinsic microstructure and can be reproducibly altered with ion-beam-induced defects. At low fluences, the critical currents in these films can be reduced by orders of magnitude without substantial changes in T_c or $\rho(300\ \mathrm{K})$. At much higher fluences, the defects cause pronounced changes in the resistive transitions, T_c goes to zero, and the films become insulating.

In this study, the critical current, I_c, was defined as the current at the break in the $I-V$ characteristic of a lithographically-defined bridge (which corresponds to developing ~ 0.5 μV between the voltage probes). Critical current densities in these oriented films are typically 10^5–10^6 A/cm^2 at 77 K. No sign of an enhancement of I_c, as reported for neutron irradiation experiments [11], was observed at the lowest fluence (1×10^{11} /cm^2). As shown in fig. 7, the decrease in J_c with 1 MeV Ne^+ ion fluence in monotonic and nonlinear. Although the fluence scale differs slightly from film to film, the shape of the curves is similar. Our results also show that the critical current in these films is much more sensitive to ion-beam-induced defects than either the T_c or the normal state resistivity. As illustrated in fig. 7, we achieved a reduction of 3 orders of magnitude in J_c at fluences less than 5×10^{13} ions/cm^2, while only increasing $\rho(300\ \mathrm{K})$ by a factor of two and maintaining T_c above 77 K.

As a first step in demonstrating that this technique might be useful for tuning the critical current of a SQUID, we irradiated selected areas of thin film structures with 2.5 μm linewidths which initially did not show any ac Josephson effect [12]. This is in contrast to the work of Koch et al. [13], who used ion irradiation to electrically isolate their SQUID patterns. A copper stencil mask with a ~ 300 μm diameter hole was used to delineate the irradiated region and the fluences of 1 MeV Ne^+ were chosen to reduce the critical current by two orders of magnitude. Indeed, the critical current was initially 10.5 mA and a fluence of 3.5×10^{13} ions/cm^2 reduced it to 0.095 mA. After irradiation, Shapiro steps appeared at a voltage spacing of 13 μV in the $I-V$ characteristics, clearly illustrating the ac Josephson effect and indicating that a weak link had been formed [14].

After investigating the effects of low ion fluences on the critical current of the films, we characterized them with respect to the destruction of superconductivity and the transition to insulating behavior at higher fluences. A series of R vs T plots at several fluences for a representative film is shown in fig. 8. Note that $\rho(T)$ increases linearly while the the onset of superconductivity moves to lower temperatures without substantial broadening of the transitions. This is reminiscent of destroying superconductivity by reducing the amplitude rather than the phase coherence of the superconducting pair wave function [15]. Since the slope of the linear region from 300 K to just above the transition at 100 K changes very little from the undamaged film to the films which received a fluence of 1.5×10^{14} ions/cm^2, we expect that the defects generated by the beam are not significantly changing the phonon spectrum, but rather are acting primarily as additional scattering centers. It is not until the spacing of these defects approaches interatomic length scales (at fluences of $\sim 2\times10^{14}$ ions/cm^2) that bulk superconductivity is destroyed in the film and the normal state resistance changes from

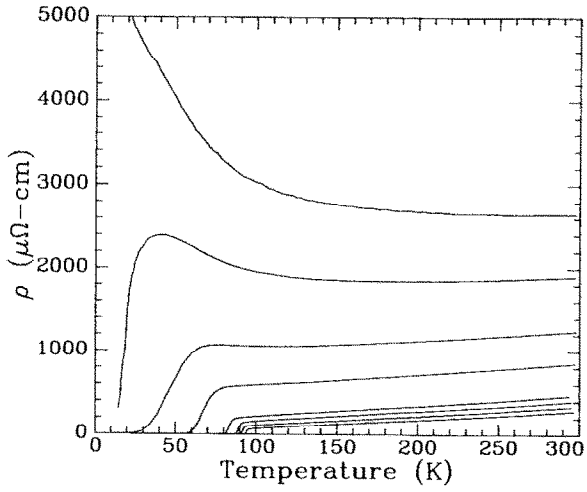

Fig. 8. Series of R vs T plots for the film from fig. 7 at higher fluences of 1 MeV Ne^+ showing the degradation of superconductivity and the transition to insulating behavior. From the bottom curve up the fluences are: 0.0, 1.0, 2.5, 4.0, 10.0, 15.0, 20.0, and 25.0×10^{13} ions/cm^2.

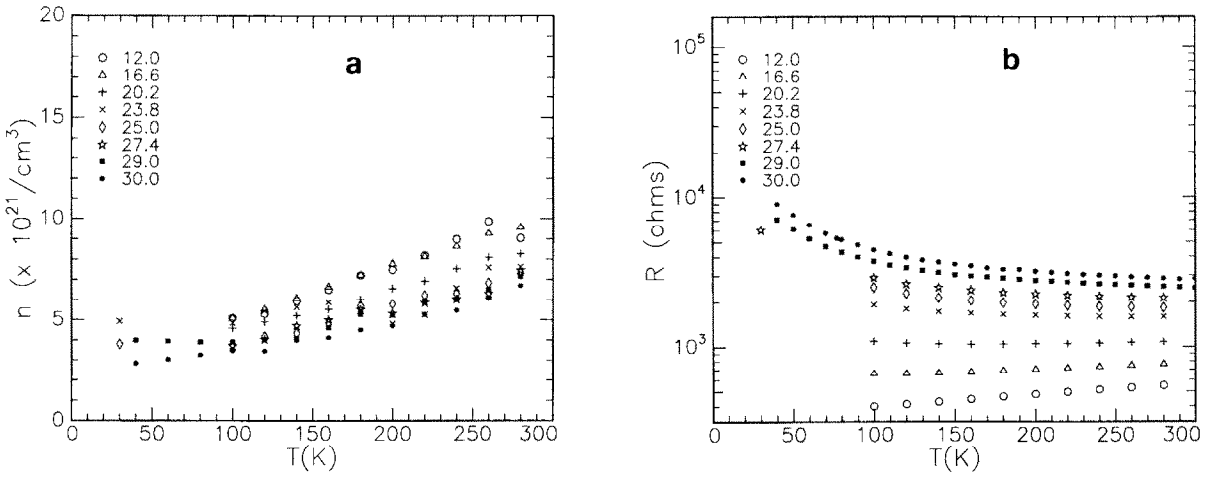

Fig. 9. (a) Inverse Hall coefficient (interpreted as the hole concentration) as a function of T for the listed fluences of 1 MeV Ne^+ (all $\times 10^{13}$ ions/cm^2). (b) R vs T plots corresponding to the Hall effect measurements shown in (a).

predominantly metal-like to semiconductor-like as seen in fig. 8.

In order to understand what the carriers were doing in the vicinity of the metal-to-insulator transition, we also measured the temperature dependence of the Hall coefficient, R_H [16]. In a simple single band metal, $1/R_H$ can be interpreted directly as the carrier density and is usually temperature-independent. Although band calculations show that $YBa_2Cu_3O_{7-\delta}$ should have a single hole band, the Hall coefficient in these films is clearly temperature-dependent, as seen in fig. 9a. This temperature dependence decreases as a function of ion fluence, however, and $1/R_H$ drops by a relatively small amount, especially at 100 K. In contrast, the resistivity of the same sample at 100 K for corresponding irradiations increases almost an order of magnitude (fig. 9b). Assuming that $1/R_H$ can be taken as a measure of the hole concentration, then the observed change in this quantity cannot account for the large change in resistivity. This implies that the mobility of the holes is being reduced instead.

5. Summary

We have reported results from a series of experiments in which ion beams were used to synthesize and modify thin films and single crystals of the high T_c oxide superconductors. Using implantation of Sr into evaporated La/Cu multilayer films followed by annealing at temperatures as low as 500 °C, naturally-capped superconducting $(La_{1-x}Sr_x)_2CuO_y$ films with onset temperatures about 40 K and broad transitions have been fabricated; however, attempts to tailor the stoichiometry of thin films of $YBa_2Cu_3O_x$ with implantation resulted in preferential sputtering of Ba. Implantation at these fluences does cause damage, so we also studied the recovery, both electrical and structural, of thin films and single crystals with a subsurface damage layer. For annealing at 800 °C, the re-ordering is close to 50% and films which had been rendered insulating by the implantation show superconducting transitions. Higher energy irradiation was used to controllably introduce defects into the films and the effect of these defects on the transport properties was monitored. Low fluences result in a large reduction in I_c before substantial changes are observed in ρ(300 K) or T_c. Higher fluences destroy the superconductivity altogether and drive the films through the metal–insulator transition. Measurements of the inverse Hall coefficient, interpreted as the hole concentration, show that the reduction in hole concentration cannot account for the large increase in resistivity produced by the ion-beam-induced defects. Therefore, we speculate that the carrier mobility is being reduced.

We would like to acknowledge useful discussions with B. Batlogg, R.J. Cava, M. Gurvitch, J.M. Poate, N.G. Stoffel, and J.S. Williams.

References

[1] R.J. Cava, B. Batlogg, R.B. van Dover, D.W. Murphy, S. Sunshine, T. Siegrist, J.P. Remeika, E.A. Reitman, S. Zahurak and G.P. Espinosa, Phys. Rev. Lett. 58 (1987) 1676.

[2] R.B. Laibowitz, R.H. Koch, P. Chaudhari and R.J. Gambino, Phys. Rev. B35 (1987) 8821.

[3] Alice E. White, K.T. Short, J.L. Batstone, D.C. Jacobson, J.M. Poate and K.W. West, Appl. Phys. Lett. 50 (1987)

19; Alice E. White, K.T. Short, R.C. Dynes, J.P. Garno and J.M. Gibson, Appl. Phys. Lett. 50 (1987) 95.
[4] J.M. Tarascon, W.R. McKinnon, L.H. Greene, G.W. Hull and E.M. Vogel, Phys. Rev. B36 (1987) 226.
[5] M. Nastasi, J.R. Tesmer, M.G. Hollander, J.F. Smith and C.J. Maggiore, J. Cryst. Growth 91 (1988) 386.
[6] A.F.J. Levi, J.M. Vandenberg, C.E. Rice, A.P. Ramirez, K.W. Baldwin, M. Anzlowar, A.E. White and K.T. Short, Appl. Phys. Lett. 1 (1988) 75; P.M. Mankiewich, J.H. Scofield, W.J. Skocpol, R.E. Howard, A.H. Dayem and E. Good, Appl. Phys. Lett. 51 (1987) 1753.
[7] N.G. Stoffel, W.A. Bonner, P.A. Morris and B.J. Wilkins, Mater. Res. Soc. Symp. Proc. 99 (1988) 507.
[8] L.F. Schneemeyer, J.V. Waszczak, T. Siegrist, R.B. van Dover, L.W. Rupp, B. Batlogg, R.J. Cava and D.W. Murphy, Nature 238 (1987) 601.
[9] K. Char, Mark Lee, R.W. Barton, A.F. Marshall, I. Bozovic, R.H. Hammond, M.R. Beasley, T.H. Geballe, A. Kapitulnik and S.S. Laderman, Phys. Rev. B38 (1988) 834.
[10] Alice E. White, K.T. Short, D.C. Jacobson, J.M. Poate, R.C. Dynes, P.M. Mankiewich, W.J. Skocpol, R.E. Howard, M. Anzlowar, K.W. Baldwin, A.F.J. Levi, J.R. Kwo, T. Hsieh and M. Hong, Phys. Rev. B37 (1988) 3755.
[11] A. Umezawa, G.W. Crabtree, J.Z. Liu, H.W. Weber, W.K. Kwok, L.H. Nunez, T.J. Moran and C.H. Sowers, Phys. Rev. B36 (1987) 7151.
[12] A.E. White, K.T. Short, R.C. Dynes, A.F.J. Levi, M. Anzlowar, K.W. Baldwin, P.A. Polakos, T.A. Fulton and L.N. Dunkleberger, Appl. Phys. Lett., 53 (1988) 1010.
[13] R.H. Koch, C.P. Umbach, G.J. Clark, P. Chaudhari and R.B. Laibowitz, Appl. Phys. Lett. 51 (1987) 200.
[14] M. Tinkham, Introduction to Superconductivity (McGraw-Hill, New York, 1985) p. 203.
[15] A.E. White, R.C. Dynes and J.P. Garno, Phys. Rev. B33 (1986) 3549; R.C. Dynes, A.E. White, J.M. Graybeal and J.P. Garno, Phys. Rev. Lett. 57 (1986) 2195.
[16] J.M. Valles, A.E. White, K.T. Short, R.C. Dynes, A.F.J. Levi, J.P. Garno, M. Anzlowar and K.W. Baldwin, to be published.